

This is an Open Access document downloaded from ORCA, Cardiff University's institutional repository: <https://orca.cardiff.ac.uk/id/eprint/130524/>

This is the author's version of a work that was submitted to / accepted for publication.

Citation for final published version:

Davies, Philip R. and Morgan, David J. 2020. Practical guide for x-ray photoelectron spectroscopy: applications to the study of catalysts. *Journal of Vacuum Science and Technology A* 38 (3) , 033204. 10.1116/1.5140747

Publishers page: <http://dx.doi.org/10.1116/1.5140747>

Please note:

Changes made as a result of publishing processes such as copy-editing, formatting and page numbers may not be reflected in this version. For the definitive version of this publication, please refer to the published source. You are advised to consult the publisher's version if you wish to cite this paper.

This version is being made available in accordance with publisher policies. See <http://orca.cf.ac.uk/policies.html> for usage policies. Copyright and moral rights for publications made available in ORCA are retained by the copyright holders.



# Practical guide for x-ray photoelectron spectroscopy: Applications to the study of catalysis

Running title: X-ray photoelectron spectroscopy for catalysts

Running Authors: Davies and Morgan

Philip R. Davies <sup>1,2</sup> and David J. Morgan <sup>1,2,a)</sup>

<sup>1</sup>Cardiff Catalysis Institute, School of Chemistry, Cardiff University, Park Place, Cardiff, CF10 3AT. UK

<sup>2</sup>HarwellXPS – EPSRC national facility for x-ray photoelectron spectroscopy, Research Complex at Harwell (RCaH), Didcot, OX11 0FE. UK

a) Electronic mail: [MorganDJ3@Cardiff.ac.uk](mailto:MorganDJ3@Cardiff.ac.uk)

X-ray photoelectron spectroscopy (XPS) has become a standard tool for the study of catalytic materials over the last two decades and with the increasing popularity of turnkey XPS systems, the analysis of these types of materials is open to an even wider audience. However, increased accessibility leads to an increase in the number of new or inexperienced practitioners, leading to erroneous data collection and interpretation. Over many years of working on a wide range of catalytic materials, we have developed procedures for the planning and execution of XPS analysis and subsequent data analysis, and this guide has been produced to help users of all levels of expertise to question their approach towards analysis and get the most out of the technique and avoiding some common pitfalls.

## I. INTRODUCTION

Heterogenous catalysis is concerned with the reaction of molecules at active sites located within the surface region of a catalytic material. The reaction itself proceeds via a series of steps including adsorption, surface diffusion, chemical reaction/rearrangement of adsorbed intermediates and finally desorption of products<sup>1-3</sup>. To aid development of such catalytic systems, modification of the surface chemical, electronic and structural properties is of extreme importance and with their inherent surface sensitivity and chemical specificity,<sup>4,5</sup> X-ray photoelectron spectroscopy (XPS) and X-ray excited Auger electron spectroscopy (XAES) have become powerful tools in the armory of the catalytic scientist.<sup>4, 6-12</sup>

Catalytic materials present some distinct challenges when it comes to surface analysis: they are often high surface area powders; usually insulating and the loading of the nanoparticulate active component can be very low (0.5 wt% or lower). XPS requires ultra-high vacuum (UHV) whilst most heterogeneous catalytic reactions take place at high pressures and temperatures, so catalytic materials are typically studied under conditions significantly different to that in which they would normally operate.<sup>2, 3</sup> Taking the simple example of a hydrated precursor, insertion in to a vacuum environment will lead to dehydration, therefore the spectra obtained would be of a dehydrated material<sup>13, 14</sup>. Nevertheless, analysis under vacuum can yield insightful information into the activity (or lack thereof) and speciation of a catalyst providing the analyst keeps in mind both the opportunities and limitations offered by the technique. Should the analyst require knowledge of samples which will not be adversely affected by vacuum, they may consider the use of near-ambient pressure (NAP-XPS) or similar.

As part of the series of practical guides for analysis,<sup>15</sup> herein we discuss some of the advantages XPS can offer to analysing catalytic materials, highlight some of the common pitfalls that may be experienced during the preparation, acquisition and interpretation of samples and data that we have experienced over many years of working within the catalytic community., and although this article may be focused on catalysis, much of the content herein is transferrable to the analysis of many other materials.

## **II. SAMPLE PREPARTION AND HISTORY**

Successful acquisition of high-quality photoemission requires significant thought toward a number of operating parameters, more of which are introduced in this paper and also referenced in the ISO 10810 standard, however at the initial level quality data begins with correct sample preparation. Industrial catalysts are typically in the form of pellets, extrudates or monoliths, whilst within an academic research environment most catalytic materials presented for analysis are powders generally comprised of metallic nanoparticles dispersed on a suitable support material such as carbon or a metal oxide. Immobilization of these powders is paramount, with poorly mounted samples potentially contaminating other samples, something especially true where large sample platens allow for the insertion of multiple sample types.

At this stage it is worth noting that each of these sample types may have its own analysis requirements. For example, homogeneity of a powdered catalyst may be assessed by running multiple aliquots from the batch, whilst an industrial catalyst may require multi-point analysis for statistical relevance to understand the active phase and its dispersion. Additionally, catalysts in either of these instances could consist a core-shell

morphology which require more detailed analysis of the photoelectron signal. We introduce these points in the sections which follow.

## A. Sample Mounting and Preparation

There are universally accepted methods of sample preparation, details of which are documented in ISO 18116 (ASTM E1078) and ISO 18117 (ASTM E1829) standards. Many of these are applicable to the surface analysis of catalysts, however each method has potential drawbacks as introduced in Table 1.

TABLE I. Common mounting methods for catalytic samples arranged in order of authors typical preference of mounting.

Mounting Method	Benefits	Potential Drawbacks
1. Pressed into tape	<ul style="list-style-type: none"> <li>• Simple</li> <li>• Cheap</li> </ul>	<ul style="list-style-type: none"> <li>• Possible silicone/organic contamination</li> <li>• Cannot pre-treat/heat samples</li> </ul>
2. Mounted into a recess	<ul style="list-style-type: none"> <li>• Simple</li> <li>• Minimizes chance of contamination</li> </ul>	<ul style="list-style-type: none"> <li>• Potential for sample loss (via turbulent flow or vibrations)</li> </ul>
3. Drop Casting on to Si	<ul style="list-style-type: none"> <li>• Smooth, thin layer</li> <li>• Negligible charging</li> <li>• In-situ treatment possible</li> </ul>	<ul style="list-style-type: none"> <li>• Organic solvent residue</li> <li>• Possibility of surface modification</li> <li>• Possible substrate peaks in spectra</li> </ul>
4. Pelletized	<ul style="list-style-type: none"> <li>• Pre-treatment possible</li> <li>• High signal intensity</li> </ul>	<ul style="list-style-type: none"> <li>• Preparation could lead to contamination from pellet press</li> <li>• Not all samples good for pressing</li> </ul>

- 5. Pressed into indium foil
    - Excellent charge neutralization
    - Considered truly UHV compatible
    - Costly (Al or Cu can be used as cheaper alternatives)
    - Potential for In signals in spectra
- 

As already mentioned, catalysts can come in many shapes and sizes and without considered preparation of the sample, XPS analysis can be difficult or give meaningless data. For example, spheres, pellets and cylindrical extrudates may have their outer surface readily analyzed, whilst catalysts presented as monoliths, miniliths, hollow extrudates and rings typically require exposure of the inner channels where the catalytic active species are located. Whilst such samples can potentially be ground into a powder, the volume of support material compared to the active species can potentially lead to significant dilution of the active species and hence low signal.

A common requirement with the analysis of catalytic materials is an in-situ treatment, such as by heating (to desorb weakly held contaminants or to initiate a material transformation) or by subjecting them to a reactive gas flow within the spectrometer, often in a linked 'catalysis cell'. Such requirements would dictate the method of sample mounting and, with reference to table 1, would preclude options (1) and (5) with options (3) or (4) considered more suitable.

Materials, such as those with significant porosity, may require prolonged periods of outgassing and such samples should be mounted and analyzed individually where possible to negate potential cross-contamination; this is especially true for materials which potentially sublime under vacuum (e.g. some halogenated materials<sup>16</sup>) although such materials may analyzed using a cooled sample stage.<sup>17</sup>

## B. Sample History

Sample history is commonly overlooked but is a significant factor that can inform the view of the analyst to the analysis requirements or to the processable data in front of them. This history should include sample preparation and treatment (e.g. a calcination or reduction sequence) and the handling and storage of samples prior to analysis.

Documenting the color of a sample prior and post analysis, such as that shown in fig 1, is recommended as materials may discolor indicating an analysis induced change, which could be pertinent to data interpretation or refinement of analysis protocols.

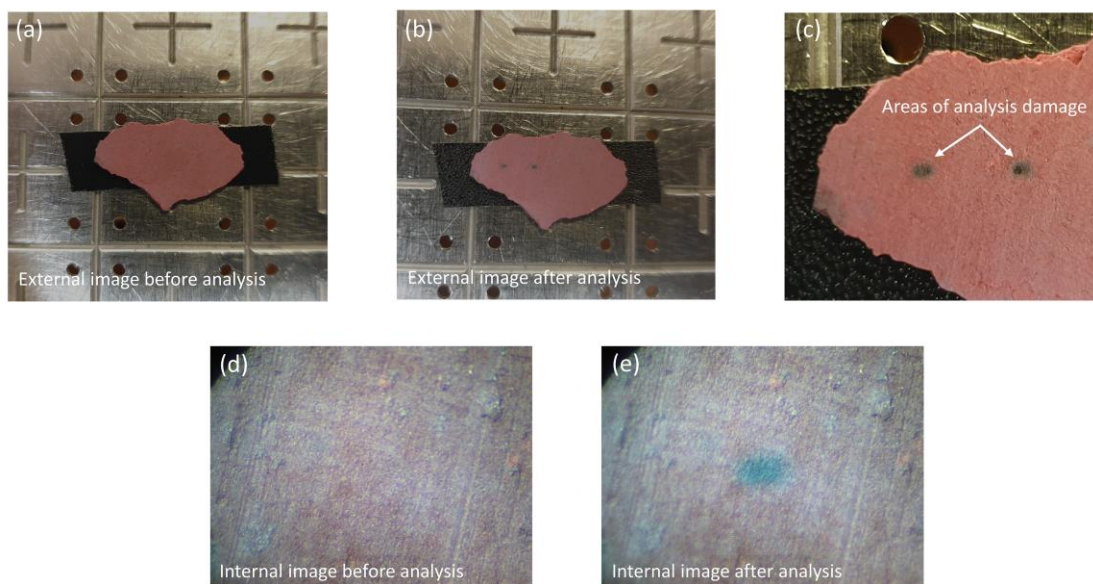


FIG. 1. Example of a color change which may be documented in the sample history. This example is of a  $\text{CrO}_3$  flake, where (a – b) show the external taken photographs of the samples before and after analysis, whilst (c) shows an enlarged area of the two analysis points. Images (d – e) show the same sample taken with the internal optical camera of the spectrometer before and after analysis.

Sample history should also include the medium in which samples were mounted, e.g. an inert atmosphere such as a glove box, or within the laboratory environment itself. Fig 2 shows an example of an iron-based Fischer-Tropsch catalyst, which has undergone partial reaction under synthesis gas at ca.250 °C and removed, under an argon atmosphere, for XPS analysis. In this figure, the lower Fe(2p) spectrum is of the sample which was mounted in the laboratory without any protective atmosphere; the time for mounting and insertion into the spectrometer was under 5 minutes, whilst the upper spectrum shows the spectrum of the same sample prepared in a glove bag purged with argon for 30 minutes prior to preparing. It is evident from these two spectra alone, that preparation in the inert atmosphere of the glove bag minimizes re-oxidation of the metallic iron compared to that of the laboratory.



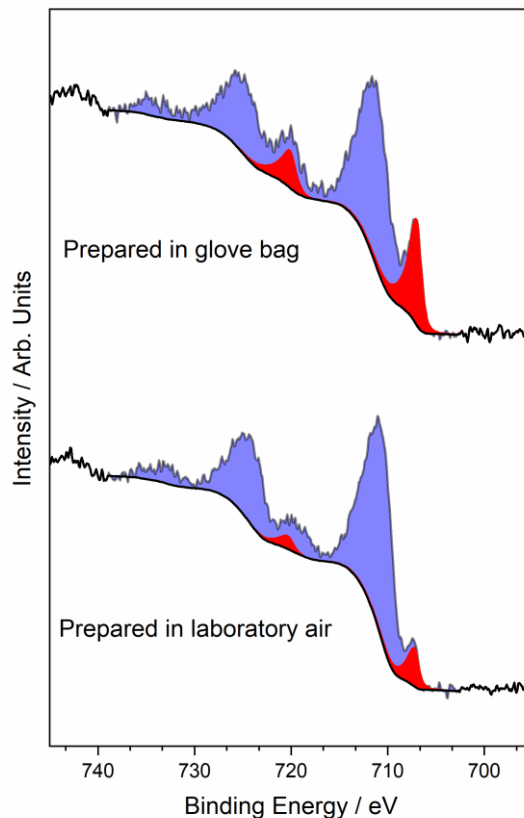


FIG. 2. Fe(2p) spectra for an Fe based Fischer-Tropsch catalysts, illustrating the difference between the same catalyst mounted in laboratory air and the same catalyst mounted in a glove bag above the load-lock of the spectrometer. The relative concentration of metallic Fe (red), with respect to the oxide (blue) is ca. 8% and 20% in the lower and upper spectra respectively. Note for simplicity Fe(III) and Fe(II) oxides have been treated as a single oxide phase in the figure.

The spectra in fig 2 clearly show that mounting in the inert atmosphere of a glove bag is more indicative of the true extent for iron reduction, which may undoubtedly be improved further where dedicated glove boxes with oxygen and moisture monitoring can be used. Nevertheless, should such a glove box not be directly attached to the

spectrometer, a weak link of transportation to the spectrometer still exists and therefore dedicated inert-gas or vacuum transfer devices should be used.

### III. EXPERIMENTAL PLANNING

The analyst may have an idea what elements are present and to be analyzed, however typical questions such as those presented in table 2 should always be asked when planning and setting out the experimental flow within the acquisition software.

TABLE 2. Typical questions the analyst should consider when preparing catalytic materials for analysis. Many of the points are discussed in the text.

Question	Possible Action
Do I know all elements present?	<ul style="list-style-type: none"> <li>• Record survey spectra and assess elements to be recorded.</li> <li>• Potentially record survey spectra on mounted replicate sample in case of x-ray induced damage?</li> </ul>
Am I looking solely for evidence of a catalytic poison such as S or Cl?	<ul style="list-style-type: none"> <li>• Record high pass energy survey spectra only</li> <li>• Record analysis sensitive elements first and again at the end.</li> </ul>
Are reducible elements present?	<ul style="list-style-type: none"> <li>• Possibly minimise number of scans or use summation of multi point analysis for better signal to noise</li> <li>• Modify x-ray power or charge neutraliser settings</li> </ul>
Can I be confident of chemical state determination from core-levels alone?	<ul style="list-style-type: none"> <li>• Record Auger lines</li> <li>• Record core-levels which exhibit multiplet splitting</li> </ul>
Do any peaks overlap?	<ul style="list-style-type: none"> <li>• Additionally, record other core-levels with sufficient photoelectron intensity. Possibly use</li> </ul>

	different excitation source
Is in-situ treatment required?	<ul style="list-style-type: none"> <li>• Select correct method of mounting</li> </ul>
Will exposure to the atmosphere modify the sample?	<ul style="list-style-type: none"> <li>• Consider use of inert transfer and/or glove box</li> </ul>
Do I need to record the valence region?	<ul style="list-style-type: none"> <li>• <i>e.g.</i> low concentrations of <math>Ti^{3+}</math> defects and Sn oxidation states may be more readily distinguished by this method<sup>18,19</sup></li> </ul>
Do I have volatile species I need to analyse?	<ul style="list-style-type: none"> <li>• Pre-cool entry and analysis stages</li> </ul>
Are the concentration of supported nanoparticles low?	<ul style="list-style-type: none"> <li>• Increase number of scans for the element in question</li> <li>• Consider running the acquisition at a higher pass energy (<i>e.g.</i> 40 eV instead of 20 eV)</li> </ul>

---

Sample modification during XPS analysis is well known in the analysis of polymers<sup>20, 21</sup>. For heterogeneous catalysts, analysis induced reduction is often observed with samples containing high valence states of Au,<sup>22, 23</sup> Pd<sup>24</sup>, Re<sup>25</sup> and Cu<sup>26</sup> amongst others<sup>27</sup>. Excellent reviews of this topic have been given by Baer *et al.*<sup>28</sup> and Thomas<sup>29</sup>, together with discussion on the mechanism of reduction. Although considered to be primarily caused by secondary electron emission, it has recently been shown that without fine-tuning the operating modes of a dual charge compensation source, there may be significant reduction in at least two important classes of catalytic materials, specifically high-valence transition metal oxides and metal-organic frameworks, an example of the improvement which can be gained is shown in fig 3 for CrO<sub>3</sub>, whilst fig 1 shows the physical changes which occur in this particular sample<sup>30</sup>. For information on optimization of charge compensation systems, a future practical guide will focus on this, but analysts are encouraged to read the ISO 19318 (ASTM E1523) standard on charge control and reporting.

Such phenomena can potentially be mitigated by the addition of rapid multi-point analysis spectra, reduced x-ray power, modified neutralizer settings or sample pre-cooling and all form part of the informed experimental approach to capture the ‘true’ surface chemistry. Table 2 attempts to summarize the questions an experimentalist should ask before undertaking analysis of a catalytic sample. It is therefore prudent to critically review acquired data in respect of unexpected chemical states.

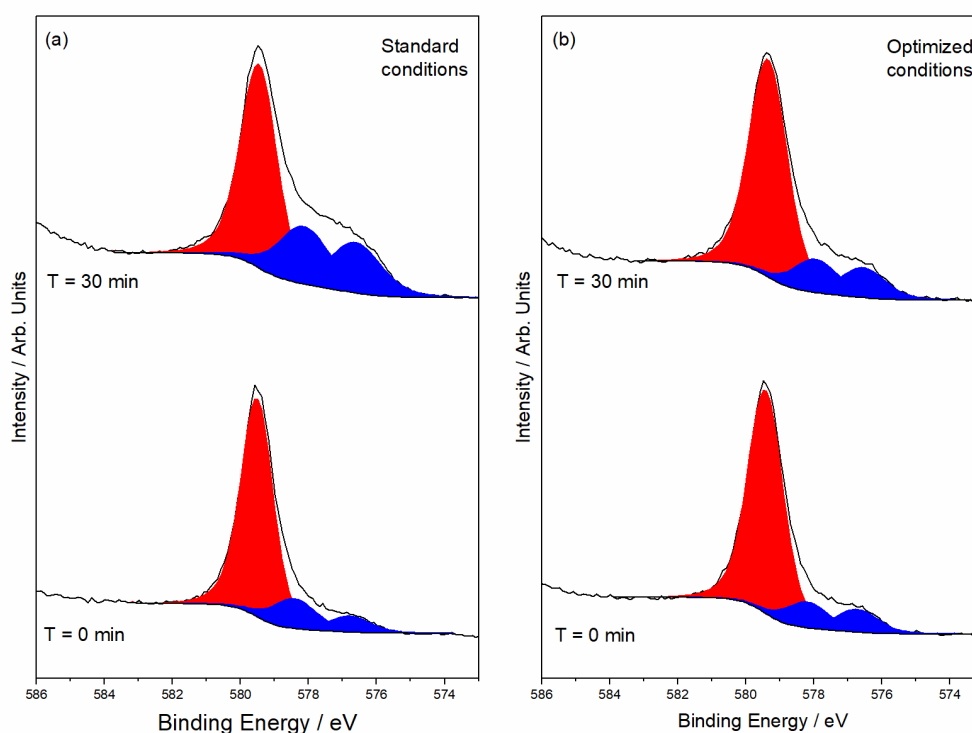


FIG. 3. Cr( $2p_{3/2}$ ) core-level spectra for  $\text{CrO}_3$  flakes taken at before ( $T = 0$  min) and after 30 min analysis, where spectra in (a) are recorded using the default neutralizer conditions and (b) are recorded using optimized charge compensation source parameters which minimizes the reduction rate. Note that although some initial  $\text{Cr}^{3+}$  reduced states are present (blue, fitted as  $\text{Cr}_2\text{O}_3$ ), the concentrations of these do not influence the observed reduction.

As highlighted in the introduction, many supported catalysts have low loadings of the active nanoparticulate phase, which depending on particle size and dispersion, will have an influence on the photoelectron signal<sup>31-33</sup>. Identification of the supported phase therefore may require prolonged acquisition times to improve signal-to-noise levels (which has a square root dependence for improvement) and may also be accompanied by a modest increase in the pass energy employed for all regions (*e.g.* 40 eV instead of 20 eV) to collect more photoelectron signal, but at the expense of a slight loss in resolution.

## **IV. BINDING ENERGIES AND SPECTRAL CALIBRATION**

### **– IS CARBON THE IDEAL CHOICE?**

The reporting of binding energies for conducting materials is straightforward, providing the user has a well characterized energy scale<sup>34</sup>, however catalytic materials are typically insulating. The choice of a well-defined and stable reference point is therefore a paramount concern to the analyst as significant shifts in the binding energy of the supported nanoparticles can occur depending on, for example, support composition, alloy formation, the interaction with the support and SMSI effects, or nanoparticle size and shape<sup>10, 35-40</sup>.

It is commonplace to calibrate to the C(1s) peak of adventitious carbon, typically assigned a value between 284.5 eV (sp<sup>2</sup> carbon) and 285 eV (sp<sup>3</sup> carbon)<sup>41</sup>, although it has long been established that this method is far from ideal<sup>40, 42-45</sup> and may also be complicated by the presence of overlapping species such as Ru<sup>46</sup>. Recently, Jacquemin *et al.*<sup>47</sup> and Greczynski and Hultman<sup>48, 49</sup> have revisited carbon charge referencing,

concluding that whilst such calibration may be suitable for comparison of similar samples, carbon referencing will always have a significant uncertainty, largely due to differences in the underlying inorganic material. Such an example of this is shown in fig 4, where the spectra show the Mg(2s)/Au(4f) and C(1s) core levels for the same Au/MgO catalyst taken before and after calcination.

The spectra are presented calibrated to the mean literature value for Mg(2s) for MgO taken from the NIST database<sup>50</sup>. Evident from the overlay spectra that the C(1s) for the calcined catalyst is shifted downward in binding energy by 0.6 eV if calibrated to the Mg(2s) support peak which may be assumed not to change. However, calcination will typically change the nature of the support, specifically altering the acid-base properties which will have an influence on the electronic environment of species on the surface, hence further elucidation of any change in the support (see for example section V, part B) may require investigation.

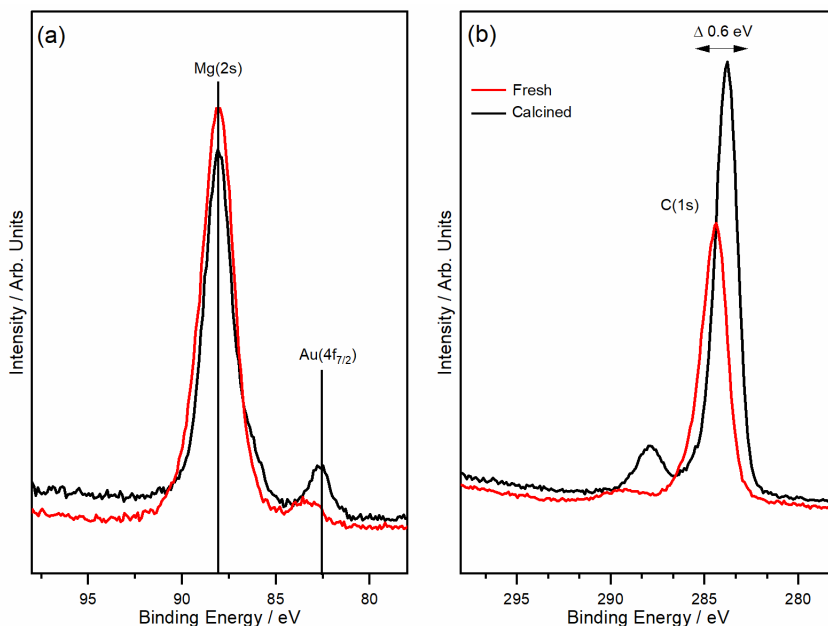


FIG 4. Fresh (red) and calcined (black) overlay of (a) Mg(2s)/Au(4f) and (b) C(1s) core-level spectra for a 1% Au/MgO catalyst indicating the caution of taking a specified peak as a constant value.

Whilst the panacea of a reliable, static calibration source for insulating samples is still far from sight, the ubiquitous nature of adventitious carbon means it remains a suitable candidate as an internal reference. However, other peaks such as O(1s) for metal oxides obtained from thin films<sup>51</sup>, or a core-level not strongly perturbed by a change in oxidation state such as Zn(2p<sub>3/2</sub>)<sup>9</sup>, Si(2p) in SiO<sub>2</sub><sup>52</sup> or the high binding energy Ce<sup>4+</sup> peak (so-called U<sup>iii</sup>, arising from a Ce<sup>4+</sup> 3d<sup>9</sup>4f<sup>0</sup>O2p<sup>6</sup> final state<sup>53, 54</sup>) for CeO<sub>2</sub><sup>55, 56</sup> may potentially be used as suitable alternatives if the analyst is unsure on the reliability of the C(1s) value. Whatever is chosen as a reference, providing there is no significant change in substrate composition and the calibration value is reported, the data obtained may be compared with similarly well-defined data in the open literature and in databases such as NIST<sup>50</sup> or Surface Science Spectra<sup>57</sup>.

## V. SPECTRAL INTERPRETATION

Photoelectron spectra contain a wealth of qualitative and quantitative information, but in some circumstances, can be extremely complex with the spectra of lanthanides prime examples<sup>58</sup>. Such complexity poses real challenges to even the most experienced analysts and one must always be on guard against commonly encountered errors such as incorrectly attributing peak asymmetry, satellite structure, multiplet splitting or screened photoemission peaks to non-stoichiometric or high oxidation states (see for example <sup>59-</sup>

<sup>66</sup>). An excellent paper on the use and misuse of curve fitting is given by Sherwood<sup>67</sup>, and we highlight some of the points raised in that paper in the following sections.

## **A. Spectral Lineshapes**

Extraction of chemical states (e.g. Pd<sup>0</sup> vs. Pd<sup>2+</sup>) from photoelectron spectra often requires spectral fitting and care must be taken to ensure the shape of the fitting function is well suited to the peak concerned; the shape of the photoelectron peak from one oxidation state cannot be assumed to be the same as that of another.

In part, such mistakes stem from the application of simple Gaussian or mixed Gaussian-Lorentzian functions to XP data to facilitate chemical state identification. Whilst these line shapes may adequately describe polymers or the simplest metal oxides, this is not always the case for metals, especially without appreciation of the relevant spin-orbit splitting or the area ratio of such peaks.

Metals have a distribution of unfilled electron levels above the Fermi level that are available for shake-up following photoemission, thus instead of observing discrete satellite features on the high binding energy side, the peak exhibits an extended tail. For a metal with a high density of states (DOS) at the Fermi level such as platinum, this effect is greatly pronounced resulting in a high degree of peak asymmetry<sup>68, 69</sup>. The effect is illustrated in fig 5 which shows the extended tail to the high binding energy side of the Pt(4f) peaks compared to those of Au



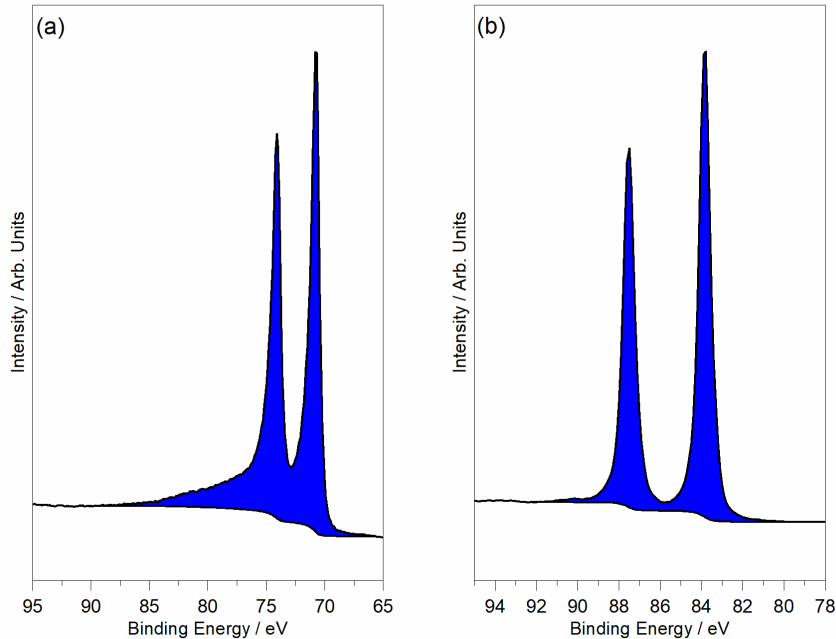


FIG 5. (a) Pt(4f) and (b) Au(4f) core-level spectra of the neighboring metals, colored to highlight the increased asymmetry for Pt over Au.

Errors which can arise from not using the appropriate asymmetric lines shapes are illustrated in fig 6, which shows the overlapping Au(4d)-Pd(3d) region for nanoparticles of metallic Au and Pd together with the presence of Pd<sup>2+</sup> supported on TS-1, a catalyst commonly used for the in-situ generation of hydrogen peroxide for oxidation reactions in academic research laboratories<sup>70-72</sup>.

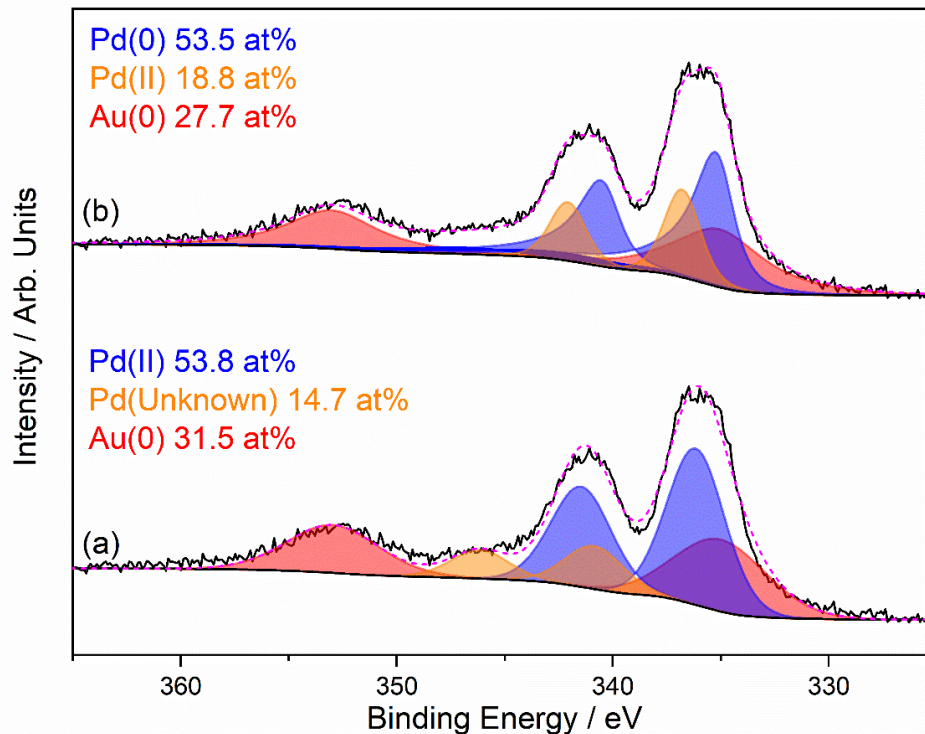


FIG 6. Pd(3d)/Au(4d) spectra of a AuPd/TS-1 catalyst, where (a) data has been incorrectly fitted using simple Gaussian-Lorentzian functions and (b) the corrected fitting based on line shapes derived from models

In fig 6(a) the spectrum has been fitted using a simple Gaussian-Lorentzian function for all peak shapes. Whilst reflecting the presence of both Pd and Au and their relative spin-orbit splitting and area ratios, the fitting has two significant issues: Firstly, the FWHM of the Pd(3d) peaks are significantly broader (*ca.* 3 eV) than expected, given the system resolution and operating conditions. Secondly, in an attempt to match the data envelope, a second Pd species has been included exhibiting an unrealistically high Pd(3d<sub>5/2</sub>) binding energy of 340.8 eV, significantly higher than any known Pd chemical state<sup>50</sup>.

Contrastingly, fig 6(b) is fitted with a single state for Au and two states of Pd (metallic and PdO) using line shapes derived from standard materials. Not only does this yield a fit more in line with the spectral envelope but, more importantly, one which reflects the catalyst structure and activity. Additionally, comparison of the Au(4d) derived atomic concentration with that of the Au(4f) derived atomic concentrations gives a confidence limit of  $\pm 0.1$  at%. The advantage of such methodology is that it allows derivation of peak shapes and constraints such as spin orbit splitting, FWHM and peak area relationships, so that models can be readily transferred between data sets and reducing uncertainty in peak fits by minimizing the number of parameters required to fit. The spectrum in fig 6(b) for example was allowed small movement in the position of the Au and Pd peaks (*ca.* 0.5 eV) from their bulk values and relaxation of the most intense peak FWHM to allow for difference in charging for example.

Such asymmetry is not only evident in metals. Graphitic carbon and conducting oxides such as RuO<sub>2</sub> and IrO<sub>2</sub> also exhibit asymmetric core-levels, with the oxides also exhibiting asymmetric O(1s) core levels<sup>46, 73-76</sup>. Furthermore, the spectral envelope can change depending levels of hydration<sup>46, 74</sup>. It is strongly recommended therefore to do a thorough search of the literature and whenever possible, for the analyst to measure their own fresh, high-purity and well characterized standard materials as a point of reference to create their own materials database.

## ***B. Chemical State Identification and Auger Lines***

Chemical state identification is typically made from binding energy assignments of spectra calibrated to a suitable reference (see section IV). However, binding energies

can be misleading, they may for example be affected by particle size<sup>39, 77-82</sup>, or the core-levels may not significantly shift between chemical states (*e.g.* Zn vs. ZnO). In such cases, the analyst may use other core-levels they have identified and recorded during their experimental design, for example the magnitude of the splitting observed for the Mn(3s) peak has often been used to elucidate the Mn oxidation state<sup>83-86</sup>, although recent studies have suggested care should be taken with such approaches<sup>87</sup>.

Greater confidence can be found in using the x-ray induced Auger lines to aid chemical state identification as described by Wagner<sup>88</sup> and utilizing Auger parameters and chemical state plots (commonly called Wagner plots)<sup>89, 90</sup>. The usefulness of such analysis in chemical state identification is widely reported and exemplified by the work of Moretti and co-workers<sup>91-94</sup>.

The differential of the C(KLL) Auger signal has found use in the analysis of carbon materials<sup>95, 96</sup>, however surface contamination and the difference in information depth of C(1s) and KLL Auger lines will increase uncertainty in the sp<sup>2</sup>/sp<sup>3</sup> ratio<sup>96, 97</sup>. More recently, Auger lines are being used in a more quantitative way<sup>98</sup>, however whilst powerful, such analysis is not always possible in practice for catalytic systems, where prolonged acquisition times are required when the active component is frequently present at very low loadings, which can potentially lead to sample modification (see section III).

Metal oxides may exhibit a complex O(1s) envelope, which can be comprised of lattice oxygen, hydroxyl, carbonate and organic species and thus complicating the analysis of absolute Auger and core-level photoelectron energies. However, an insight into the oxides surface electronic properties can be elucidated from the O(KLL) Auger lines and the associated Auger parameter ( $\alpha$ ), where  $\alpha$  = Kinetic energy (Auger

line)+Binding energy (photoemission line), since the emission is from a common core-level. Relative to gaseous water ( $\alpha = 1038.5 \text{ eV}^{99}$ ), increasing values of  $\alpha$  with decreasing separation of the O  $\text{KL}_{23}\text{L}_{23}$  and O  $\text{KL}_1\text{L}_{23}$  signals indicate increasing surface polarizability and hence facilitates a quantitative measurement of Lewis basicity<sup>99-103</sup>.

### **C. *Fresh, in-situ and Post-Mortem Analysis of Samples***

The majority of data presented at conferences or within peer reviewed journals, primarily focuses on the ‘fresh’ state of a catalyst, yielding valuable information on the initial chemical states on the surface. However, in-situ treatments, ‘pseudo in-situ’ (where the sample is removed from the catalytic reactor at different intervals for analysis) and post-mortem analysis of catalysts can yield significant insights in to the active species or deactivation of a catalyst, be it through formation of a particular chemical state<sup>11, 104</sup>, leaching<sup>105, 106</sup>, sintering<sup>107, 108</sup>, formation of strongly bound species<sup>8, 109</sup> or coke formation<sup>110, 111</sup>.

To exemplify this, we briefly compare the fresh and post-mortem analysis of a  $\text{Fe}_x\text{Cr}_y\text{O}_z$  catalyst used for propane dehydrogenation, fig 7.

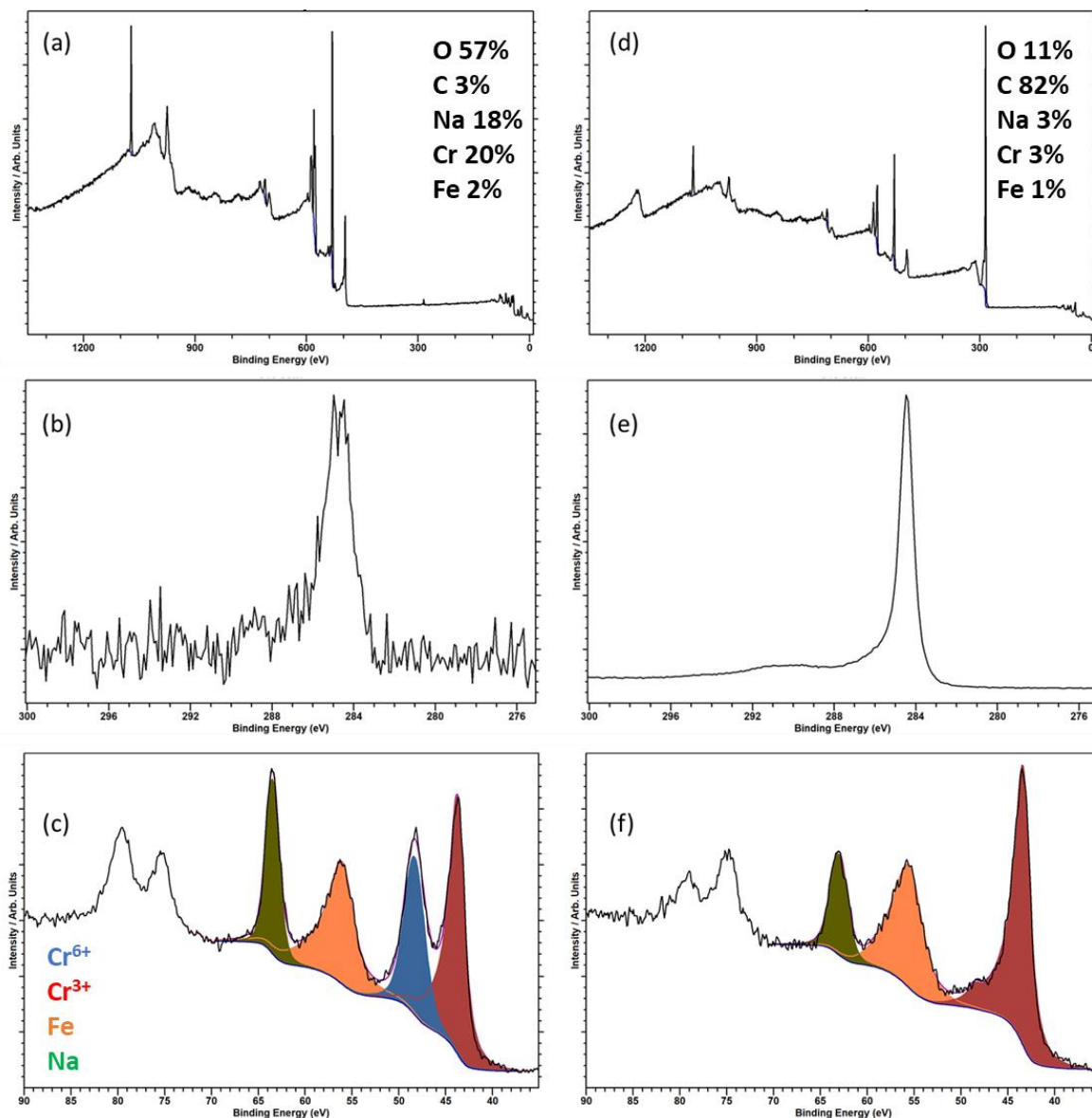


FIG 7. Survey, C(1s) and Cr(3p)/Fe(3p)/Na(2s) core-level spectra for (a, b, c) fresh catalyst and (d, e, f) used catalyst respectively

For the fresh catalyst, it is evident from fig 7(c) that both  $\text{Cr}^{6+}$  and  $\text{Cr}^{3+}$  species are present, whereas the used catalyst possesses only  $\text{Cr}^{3+}$  (fig 7(f)); note here the high kinetic energy (low binding energy) peaks have been recorded in addition to the standard core-levels (e.g. Cr(2p) and Fe(2p)) since the escape depth of these photoelectrons will be similar and less affected by the attenuating carbon overlayer. For some materials, such as

uranium, analysis of these high kinetic energy lines proves more beneficial in determination of oxidation state than the main core-lines<sup>112</sup>.

Moreover, for the fresh catalyst the carbon is adventitious and only 3% of the total elemental concentration, whereas for the spent catalyst carbon accounts for over 80% of the total concentration and, as shown in fig 7(e), exhibits a shape typical of graphitic carbon<sup>97</sup> and indicating severe coking during reaction. From fig 7(a & d) the relative amounts of Cr, Fe and Na have also changed, potentially indicating sintering.

Understanding that coking is occurring in such catalysts is important as it allows tuning of the Cr/Fe content and chemical states to influence selectivity to propene formation and limit the rate of coke formation<sup>113</sup>. With analysis of the XAES D-parameter<sup>95,96</sup> or *via* the advent of coincident Raman spectroscopy on XPS systems, further insights into the aromaticity of the coke may be examined<sup>114,115</sup>.

#### ***D. Determination of Particle Size and Dispersion***

One of the biggest factors in the activity of catalysis is particle size, which in turn affects dispersion. Whilst X-ray diffraction (XRD) or chemisorption methods are used for particle size determination, both techniques have limitations; the former relies on long-range order to obtain crystals of sufficient size for Bragg diffraction (*ca.* 5 nm), whereas in the latter geometric factors of the particles are typically ignored. The surface sensitivity of XPS, means it is ideally suited to recognizing how well particles are dispersed over a support material. If one assumes the case of two catalysts with an identical amount of material in the supported phase, then for a case where very small particles are present the surface is to a large extent covered by the nanoparticles. For

where the particles are larger however, the dispersion is poor and hence if we ratio the photoelectron signal from the particle ( $I_p$ ) to that of the support ( $I_s$ ), then we have a case where  $I_p/I_s$  is low for poorly dispersed particles and high for well dispersed particles.

Extending this Kerkhof and Moulijn<sup>32</sup> proposed a simple model (later simplified by León<sup>116</sup>) for the determination of particle sizes, which uses the aforementioned ratio for a quantitative estimation of the dispersion by modelling a supported catalyst as a stack of sheets with cuboid crystals representing support particles and has been shown to give excellent agreement with sizes derived from chemisorption measurements. A second method, relying on the intensity ratio for two core-levels of significantly different kinetic energies was proposed by Davis<sup>117</sup> and is independent from the catalyst surface area and loading. This method, which is especially suited to systems with monochromatic Ag sources for accessing higher binding energy photoemission lines, has been successfully applied to a number of systems<sup>117-120</sup>, providing the particles sizes are below *ca.*  $2\lambda$  (where  $\lambda$  is the electron inelastic mean free path), although contamination overlayers which would attenuate lower kinetic energy signals would limit accuracy, however such an analysis requirement would feed in to the experimental planning stage.

Other methods to extract particle size information include well-defined changes in binding energy and analysis of energy-loss electrons within the photoelectron background<sup>80, 121</sup>. Such particle size information from XPS has allowed correlation with the catalytic turnover frequency<sup>122-124</sup>.

Many supported particles may be of a core-shell, or similar, morphology, and will therefore have photoelectron intensity ratios influenced by the core-shell morphology. Shard et al. have developed models to account for such morphologies and but accuracy



may be there is a significant difference in the kinetic energies of the core and shell materials are widely different<sup>125</sup>. Such spectra may also be modelled through the use of simulation software, such as SESSA<sup>126</sup> to evaluate the inner structure of core-shell morphologies<sup>127, 128</sup>.

For all the models in this section, the theory and mathematics of each method is beyond the scope of this paper and readers are encouraged to review the relevant supplied references.

### ***E. High Energy XPS (HAXPES) in Catalysis***

Whilst higher energy sources have been available for many years<sup>129-133</sup>, their wider use has been somewhat precluded by primarily wide-scale availability, broader linewidths and decreased elemental sensitivity to orbitals conventionally studied with Al/Mg radiation<sup>134</sup>. Many instrument manufacturers now routinely offer monochromatic Ag or Cr sources, their use is still somewhat in their infancy in catalysis for lab-based systems, with many studies still reliant on synchrotron radiation<sup>135, 136</sup>.

Despite the lower sensitivity to many orbitals routinely analyzed using Al/Mg excitation for higher photon energy sources, the depth information which may be obtained by relatively simple measurements can greatly enhance information in, for example zeolites and 2D materials, or facilitate extraction of layer information via Tougaard analysis<sup>137-139</sup>.

Of course, the question ‘why use such lab based HAXPES sources in the analysis of catalytic materials since catalysis is a surface phenomenon’ can be raised. We have already highlighted the use in particle size determination (section V, part D), however it

should be noted both sub-surface and bulk compositions can influence surface properties so being able to gauge such information is useful. Additionally, using such sources on coked material, such as those shown in fig 7, can facilitate the analysis of the buried interfacial chemistry.

## **VI. CONCLUSIVE SUMMARY**

XPS is a lynchpin in the analysis of catalytic materials allowing quantitative chemical speciation and the ability to probe the electronic structure and the morphological character of a material. It has the power to differentiate chemical states, obtain molar ratios, elucidate catalytic dispersion and particle size when results from other techniques may be obtuse.

Without considered planning however, XPS measurements can yield misleading results due to poorly informed analysis protocols or data misinterpretation. It is evident the information to be obtained from each analysis will be different since the questions to be answered for each sample will vary. Definition of the questions to be answered by means of the analysis beforehand help achieve an informed analysis protocol for each sample which we hope have been brought to attention within this paper.

## **ACKNOWLEDGMENTS**

The authors wish to express their sincere thanks to all our mentors, colleagues and co-workers who, over many years, have facilitated the great science to which we have been part of.

Some of the work included herein has been generated through our provision of the EPSRC National Facility for Photoelectron Spectroscopy (HarwellXPS), operated by Cardiff University and UCL under contract number PR16195.

<sup>1</sup>M. S. Spencer, *Fundamental Principles*, in: M.V. Twigg (Ed.) *Catalyst Handbook*, CRC Press, 1989.

<sup>2</sup>B. C. Gates, *Catalytic Chemistry*, (John Wiley & Sons, Ltd, 1992).

<sup>3</sup>J. Hagen, *Industrial Catalysis: A Practical Approach*, (Wiley-VCH, Weinheim, Germany, 2015).

<sup>4</sup>A. M. Venezia, *Catal. Today* **77**, 359 (2003).

<sup>5</sup>J. F. Watts, J. Wolstenholme, *An Introduction to Surface Analysis by XPS and AES*, 2nd Edition ed., (John Wiley & Sons, Ltd, Chichester, UK, 2003).

<sup>6</sup>J. H. Carter, P. M. Shah, E. Nowicka, S. J. Freakley, D. J. Morgan, S. Golunski, G. J. Hutchings, *Front. Chem.* **7**, 443 (2019).

<sup>7</sup>G. W. Coulston, E. A. Thompson, N. Herron, *J. Catal.* **163**, 122 (1996).

<sup>8</sup>D. R. Jones, S. Iqbal, P. J. Miedziak, D. J. Morgan, J. K. Edwards, Q. He, G. J. Hutchings, *Top. Catal.* **61**, 833 (2018).

<sup>9</sup>E. Nowicka, S. M. Althahban, Y. Luo, R. Kriegel, G. Shaw, D. J. Morgan, Q. He, M. Watanabe, M. Armbrüster, C. J. Kiely, G. J. Hutchings, *Catal. Sci. Technol.* **8**, 5848 (2018).

- <sup>10</sup>T. M. Nyathi, N. Fischer, A. P. E. York, D. J. Morgan, G. J. Hutchings, E. K. Gibson, P. P. Wells, C. R. A. Catlow, M. Claeys, *ACS Catal.* **7**, 7166 (2019).
- <sup>11</sup>X. Liu, M. Conte, D. Elias, L. Lu, D. J. Morgan, S. J. Freakley, P. Johnston, C. J. Kiely, G. J. Hutchings, *Catal. Sci. Technol.* **6**, 5144 (2016).
- <sup>12</sup>G. Malta, S. A. Kondrat, S. J. Freakley, C. J. Davies, L. Lu, S. Dawson, A. Thetford, E. K. Gibson, D. J. Morgan, W. Jones, P. P. Wells, P. Johnston, C. R. Catlow, C. J. Kiely, G. J. Hutchings, *Science* **355**, 1399 (2017).
- <sup>13</sup>M. Schindler, F. C. Hawthorne, M. S. Freund, P. C. Burns, *Geochim. Cosmochim. Acta* **73**, 2471 (2009).
- <sup>14</sup>D. J. Tobler, J. D. Rodriguez-Blanco, K. Dideriksen, N. Bovet, K. K. Sand, S. L. S. Stipp, *Advanced Functional Materials* **25**, 3081 (2015).
- <sup>15</sup>D. R. Baer, K. Artyushkova, C. Richard Brundle, J. E. Castle, M. H. Engelhard, K. J. Gaskell, J. T. Grant, R. T. Haasch, M. R. Linford, C. J. Powell, A. G. Shard, P. M. A. Sherwood, V. S. Smentkowski, *J. Vac. Sci. Technol., A* **37**, (2019).
- <sup>16</sup>I. A. Leenson, *J. Chem. Edu.* **82**, (2005).
- <sup>17</sup>Y. Mikhlin, A. Karacharov, Y. Tomashevich, A. Shchukarev, *J. Electron Spectrosc. Relat. Phenom.* **206**, 65 (2016).
- <sup>18</sup>N. Tsud, V. Johánek, I. Stará, K. Veltruská, V. Matolín, *Thin Solid Films* **391**, 204 (2001).
- <sup>19</sup>X. Chen, L. Liu, Z. Liu, M. A. Marcus, W. C. Wang, N. A. Oyler, M. E. Grass, B. Mao, P. A. Glans, P. Y. Yu, J. Guo, S. S. Mao, *Sci. Rep.* **3**, 1510 (2013).

- <sup>20</sup>G. Beamson, D. Briggs, *High Resolution XPS of Organic Polymers: The Scienta ESCA300 Database*, (Wiley, Chichester, 1992).
- <sup>21</sup>M. Engelhard, D. Baer, S. Lea, *Surf. Sci. Spectra* **10**, 80 (2003).
- <sup>22</sup>Y. Y. Fong, B. R. Visser, J. R. Gascooke, B. C. Cowie, L. Thomsen, G. F. Metha, M. A. Buntine, H. H. Harris, *Langmuir* **27**, 8099 (2011).
- <sup>23</sup>M. Conte, C. J. Davies, D. J. Morgan, A. F. Carley, P. Johnston, G. J. Hutchings, *Catal. Lett.* **144**, 1 (2013).
- <sup>24</sup>T. H. Fleisch, G. J. Mains, *J. Phys. Chem.* **90**, 5317 (1986).
- <sup>25</sup>S. Iqbal, M. L. Shoji, D. J. Morgan, *Surf. Interface Anal.* **49**, 223 (2017).
- <sup>26</sup>M. C. Biesinger, L. W. M. Lau, A. R. Gerson, R. S. C. Smart, *Appl. Surf. Sci.* **257**, 887 (2010).
- <sup>27</sup>Ş. Süzer, *Appl. Spectrosc.* **54**, 1716 (2016).
- <sup>28</sup>D. Baer, M. Engelhard, D. Gaspar, S. Lea, *Beam Effects During AES and XPS Analysis*, in: D. Briggs, J.T. Grant (Eds.) *Surface Analysis by Auger and X-ray Photoelectron Spectroscopy*, IM Publications LLP, Chichester, UK, 2003.
- <sup>29</sup>J. H. III Thomas, *Photon Beam Damage and Charging at Solid Surfaces*, in: A.W. Czanderna, T.E. Madey, C.J. Powell (Eds.) *Beam Effects, Surface Topography and Depth Profiling in Surface Analysis*, Plenum Press, New York, 1998, pp. 1.
- <sup>30</sup>L. Edwards, P. Mack, D. J. Morgan, *Surf. Interface Anal.* **51**, 925 (2019).
- <sup>31</sup>V. Di Castro, C. Furlani, M. Gargano, N. Ravasio, M. Rossi, *J. Electron Spectrosc. Relat. Phenom.* **52**, 415 (1990).

- <sup>32</sup>F. P. J. M. Kerkhof, J. A. Moulijn, *J. Phys. Chem.* **83**, 1612 (1979).
- <sup>33</sup>J. W. Niemantsverdriet, *Spectroscopy in Catalysis*, 3rd Edition ed., (Wiley-VCH Verlag GmbH & Co, 2007).
- <sup>34</sup>C. J. Powell, *J. Electron Spectrosc. Relat. Phenom.* *In Press*,  
<http://dx.doi.org/10.1016/j.elspec.2018.11.007> (2019).
- <sup>35</sup>A. Fernández, A. Caballero, A. R. González-Elipse, *Surf. Interface Anal.* **18**, 392 (1992).
- <sup>36</sup>A. Frydman, D. G. Castner, M. Schmal, C. T. Campbell, *J. Catal.* **152**, 164 (1995).
- <sup>37</sup>N. Kruse, S. Chenakin, *Appl. Catal., A* **391**, 367 (2011).
- <sup>38</sup>A. Lewera, L. Timperman, A. Roguska, N. Alonso-Vante, *J. Phys. Chem. C.* **115**, 20153 (2011).
- <sup>39</sup>K. Luo, D. Y. Kim, D. W. Goodman, *J. Mol. Catal. A: Chem.* **167**, 191 (2001).
- <sup>40</sup>R. Radnik, C. Mohr, P. Claus, *Phys Chem Chem Phys* **5**, 172 (2003).
- <sup>41</sup>B. V. Crist, *J. Electron Spectrosc. Relat. Phenom.* **231**, 75 (2019).
- <sup>42</sup>R. Blume, D. Rosenthal, J.-P. Tessonnier, H. Li, A. Knop-Gericke, R. Schlögl, *ChemCatChem* **7**, 2871 (2015).
- <sup>43</sup>Böse O, E. Kemnitz, A. Lippitz, W. E. S. Unger, *Fresenius' J. Anal. Chem.* **358**, 175 (1997).
- <sup>44</sup>S. Kohiki, K. Oki, *J. Electron Spectrosc. Relat. Phenom.* **33**, 375 (1984).
- <sup>45</sup>W. E. S. Unger, T. Gross, O. Bose, U. Gelius, T. Fritz, A. Lippitz, *Surf. Interface Anal.* **29**, 535 (2000).

- <sup>46</sup>D. J. Morgan, Surf. Interface Anal. **47**, 1072 (2015).
- <sup>47</sup>M. Jacquemin, M. J. Genet, E. M. Gaigneaux, D. P. Debecker, ChemPhysChem **14**, 3618 (2013).
- <sup>48</sup>G. Greczynski, L. Hultman, ChemPhysChem **18**, 1507 (2017).
- <sup>49</sup>G. Greczynski, L. Hultman, Appl. Surf. Sci. **451**, 99 (2018).
- <sup>50</sup>*NIST X-ray Photoelectron Spectroscopy Database, Version 4.1 (National Institute of Standards and Technology, Gaithersburg, 2012)*, <http://srdata.nist.gov/xps/>.
- <sup>51</sup>A. K. Bhattacharya, D. R. Pyke, R. Reynolds, G. S. Walker, A. K. Bhattacharya, J. Mater. Sci. Lett. **16**, 1 (1997).
- <sup>52</sup>M. J. Remy, M. J. Genet, G. Poncelet, P. F. Lardinois, P. P. Notte, J. Phys. Chem. **96**, 2614 (1992).
- <sup>53</sup>E. Paparazzo, G. M. Ingo, N. Zacchetti, Journal of Vacuum Science & Technology A: Vacuum, Surfaces, and Films **9**, 1416 (1991).
- <sup>54</sup>M. M. Natile, A. Glisenti, Surf. Sci. Spectra **13**, 17 (2006).
- <sup>55</sup>C. Barth, C. Laffon, R. Olbrich, A. Ranguis, P. Parent, M. Reichling, Sci. Rep. **6**, 21165 (2016).
- <sup>56</sup>D.-G. Cheng, M. Chong, F. Chen, X. Zhan, Catal. Lett. **120**, 82 (2007).
- <sup>57</sup>*Surface Science Spectra*, <http://avs.scitation.org/journal/sss>.
- <sup>58</sup>Y. A. Teterin, A. Y. Teterin, Russ. Chem. Rev. **71**, 347 (2002).
- <sup>59</sup>J. Balcerzak, W. Redzynia, J. Tyczkowski, Appl. Surf. Sci. **426**, 852 (2017).

- <sup>60</sup>B. Desalegn, M. Megharaj, Z. Chen, R. Naidu, Heliyon **5**, e01750 (2019).
- <sup>61</sup>J. H. Kim, J. Y. Cheon, T. J. Shin, J. Y. Park, S. H. Joo, Carbon **101**, 449 (2016).
- <sup>62</sup>K. W. Brinkley, M. Burkholder, A. R. Siamaki, K. Belecki, B. F. Gupton, Green Process. Synth. **4**, 241 (2015).
- <sup>63</sup>I. Roger, R. Moca, H. N. Miras, K. G. Crawford, D. A. J. Moran, A. Y. Ganin, M. D. Symes, J. Mater. Chem. A **5**, 1472 (2017).
- <sup>64</sup>A. M. García, V. L. Budarin, Y. Zhou, M. De bruyn, A. J. Hunt, L. Lari, V. K. Lazarov, H. J. Salavagione, E. Morales, G. J. Ellis, J. H. Clark, P. S. Shuttleworth, J. Mater. Chem. A **6**, 1119 (2018).
- <sup>65</sup>M. Zannotti, C. J. Wood, G. H. Summers, L. A. Stevens, M. R. Hall, C. E. Snape, R. Giovannetti, E. A. Gibson, ACS Appl Mater Interfaces **7**, 24556 (2015).
- <sup>66</sup>N. Poldme, L. O'Reilly, I. Fletcher, J. Portoles, I. V. Sazanovich, M. Towrie, C. Long, J. G. Vos, M. T. Pryce, E. A. Gibson, Chem Sci **10**, 99 (2019).
- <sup>67</sup>P. M. A. Sherwood, Surf. Interface Anal. **51**, 589 (2019).
- <sup>68</sup>D. Briggs, *XPS: Basic Principles, Spectral Features and Qualitative Analysis*, in: D. Briggs, J.T. Grant (Eds.) Surface Analysis by Auger and X-ray Photoelectron Spectroscopy, IM Publications LLP, Chichester, UK, 2003.
- <sup>69</sup>H. Höchst, S. Hüfner, A. Goldmann, Phys. Lett. A. **57**, 265 (1976).
- <sup>70</sup>R. J. Lewis, K. Ueura, Y. Fukuta, S. J. Freakley, L. Kang, R. Wang, Q. He, J. K. Edwards, D. J. Morgan, Y. Yamamoto, G. J. Hutchings, ChemCatChem **11**, 1673 (2019).
- <sup>71</sup>V. R. Choudhary, N. S. Patil, S. K. Bhargava, Catal. Lett. **89**, 55 (2003).



- <sup>72</sup>D. J. Robinson, L. Davies, N. McGuire, D. F. Lee, P. McMorn, J. Willock, G. W. Watson, P. C. Bulman Page, D. Bethell, J. Hutchings, *Phys Chem Chem Phys* **2**, 1523 (2000).
- <sup>73</sup>P. A. Cox, J. B. Goodenough, P. J. Tavener, D. Telles, R. G. Egdell, *J. Solid State Chem.* **62**, 360 (1986).
- <sup>74</sup>S. J. Freakley, J. Ruiz-Esquiús, D. J. Morgan, *Surf. Interface Anal.* **49**, 794 (2017).
- <sup>75</sup>Y. J. Kim, Y. Gao, S. A. Chambers, *Appl. Surf. Sci.* **120**, 250 (1997).
- <sup>76</sup>G. K. Wertheim, H. J. Guggenheim, *Phys. Rev. B.* **22**, 4680 (1980).
- <sup>77</sup>I. Aruna, B. R. Mehta, L. K. Malhotra, S. M. Shivaprasad, *J. Appl. Phys.* **104**, (2008).
- <sup>78</sup>B. Balamurugan, T. Maruyama, *Appl. Phys. Lett.* **89**, (2006).
- <sup>79</sup>A. F. Carley, L. A. Dollard, P. R. Norman, C. Pottage, M. W. Roberts, *J. Electron Spectrosc. Relat. Phenom.* **98**, 223 (1999).
- <sup>80</sup>A. R. Gonzalez-Elipe, G. Munuera, J. P. Espinos, *Surf. Interface Anal.* **16**, 375 (1990).
- <sup>81</sup>G. Lassaletta, A. Fernandez, J. P. Espinos, A. R. Gonzalez-Elipe, *J. Phys. Chem.* **99**, 1484 (1995).
- <sup>82</sup>J. Morales, A. Caballero, J. P. Holgado, J. P. Espinós, A. R. González-Elipe, *J. Phys. Chem. B.* **106**, 10185 (2002).
- <sup>83</sup>J. L. Junta, M. F. Hochella, *Geochim. Cosmochim. Acta* **58**, 4985 (1994).
- <sup>84</sup>D. Banerjee, H. W. Nesbitt, *Geochim. Cosmochim. Acta* **63**, 3025 (1999).
- <sup>85</sup>D. Banerjee, H. W. Nesbitt, *Geochim. Cosmochim. Acta* **63**, 1671 (1999).

- <sup>86</sup>D. Banerjee, H. W. Nesbitt, *Geochim. Cosmochim. Acta* **65**, 1703 (2001).
- <sup>87</sup>E. S. Ilton, J. E. Post, P. J. Heaney, F. T. Ling, S. N. Kerisit, *Appl. Surf. Sci.* **366**, 475 (2016).
- <sup>88</sup>C. D. Wagner, *Anal. Chem.* **44**, 967 (2002).
- <sup>89</sup>C. D. Wagner, L. H. Gale, R. H. Raymond, *Anal. Chem.* **51**, 466 (2002).
- <sup>90</sup>C. D. Wagner, *Faraday Discuss. Chem. Soc.* **60**, (1975).
- <sup>91</sup>G. Moretti, F. Filippone, M. Satta, *Surf. Interface Anal.* **31**, 249 (2001).
- <sup>92</sup>G. Moretti, *J. Electron Spectrosc. Relat. Phenom.* **95**, 95 (1998).
- <sup>93</sup>G. Moretti, *Surf. Sci.* **618**, 3 (2013).
- <sup>94</sup>G. Moretti, A. Palma, E. Paparazzo, M. Satta, *Surf. Sci.* **646**, 298 (2016).
- <sup>95</sup>J. C. Lascovich, S. Scaglione, *Appl. Surf. Sci.* **78**, 17 (1994).
- <sup>96</sup>B. Lesiak, L. Kövér, J. Tóth, J. Zemek, P. Jiricek, A. Kromka, N. Rangam, *Appl. Surf. Sci.* **452**, 223 (2018).
- <sup>97</sup>D. J. Morgan, *Surf. Sci. Spectra* **24**, 024003 (2017).
- <sup>98</sup>M. C. Biesinger, *Surf. Interface Anal.* **49**, 1325 (2017).
- <sup>99</sup>J. A. D. Matthew, S. Parker, *J. Electron Spectrosc. Relat. Phenom.* **85**, 175 (1997).
- <sup>100</sup>J. M. Montero, P. Gai, K. Wilson, A. F. Lee, *Green Chem.* **11**, 265 (2009).
- <sup>101</sup>G. Moretti, *J. Electron Spectrosc. Relat. Phenom.* **58**, 105 (1992).
- <sup>102</sup>P. Ascarelli, G. Moretti, *Surf. Interface Anal.* **7**, 8 (1985).

- <sup>103</sup>J. van den Brand, P. C. Snijders, W. G. Sloof, H. Terryn, J. H. W. de Wit, *J. Phys. Chem. B.* **108**, 6017 (2004).
- <sup>104</sup>G. Malta, S. J. Freakley, S. A. Kondrat, G. J. Hutchings, *Chem. Commun.* **53**, 11733 (2017).
- <sup>105</sup>Y. Ji, S. Jain, R. J. Davis, *J. Phys. Chem. B* **109**, 17232 (2005).
- <sup>106</sup>A. A. Youzbashi, S. G. Dixit, *Metall. Mater. Trans. B* **22**, 775 (1991).
- <sup>107</sup>S. Wodiunig, J. M. Keel, T. S. E. Wilson, F. W. Zemichael, R. M. Lambert, *Catal. Lett.* **87**, 1 (2003).
- <sup>108</sup>Y. Niu, P. Schlexer, B. Sebok, I. Chorkendorff, G. Pacchioni, R. E. Palmer, *Nanoscale* **10**, 2363 (2018).
- <sup>109</sup>S. Iqbal, S. A. Kondrat, D. R. Jones, D. C. Schoenmakers, J. K. Edwards, L. Lu, B. R. Yeo, P. P. Wells, E. K. Gibson, D. J. Morgan, C. J. Kiely, G. J. Hutchings, *ACS Catal.* **5**, 5047 (2015).
- <sup>110</sup>B. Sexton, *J. Catal.* **109**, 126 (1988).
- <sup>111</sup>B. S. Liu, L. Jiang, H. Sun, C. T. Au, *Appl. Surf. Sci.* **253**, 5092 (2007).
- <sup>112</sup>E. S. Ilton, Y. Du, J. E. Stubbs, P. J. Eng, A. M. Chaka, J. R. Bargar, C. J. Nelin, P. S. Bagus, *Phys Chem Chem Phys* **19**, 30473 (2017).
- <sup>113</sup>O. F. Gorrioz, V. Cortes Corberan, J. L. G. Fierro, *Ind. Eng. Chem. Res.* **31**, 2670 (1992).
- <sup>114</sup>P. C. Stair, *Adv. Catal.* **51**, 75 (2007).

- <sup>115</sup>S. R. Bare, F. D. Vila, M. E. Charochak, S. Prabhakar, W. J. Bradley, C. Jaye, D. A. Fischer, S. T. Hayashi, S. A. Bradley, J. J. Rehr, *ACS Catal.* **7**, 1452 (2017).
- <sup>116</sup>V. León, *Surf. Sci.* **339**, L931 (1995).
- <sup>117</sup>S. M. Davis, *J. Catal.* **117**, 432 (1989).
- <sup>118</sup>R. Wojcieszak, A. Karelavic, E. M. Gaigneaux, P. Ruiz, *Catal. Sci. Technol.* **4**, 3298 (2014).
- <sup>119</sup>M. Y. Smirnov, A. V. Kalinkin, A. V. Bukhtiyarov, I. P. Prosvirin, V. I. Bukhtiyarov, *J. Phys. Chem. C.* **120**, 10419 (2016).
- <sup>120</sup>M. N. Ghazzal, R. Wojcieszak, G. Raj, E. M. Gaigneaux, *Beilstein J. Nanotechnol.* **5**, 68 (2014).
- <sup>121</sup>S. Hajati, V. Zaporozhchenko, F. Faupel, S. Tougaard, *Surf. Sci.* **601**, 3261 (2007).
- <sup>122</sup>L. V. Nosova, M. V. Stenin, Y. N. Nogin, Y. A. Ryndin, *Appl. Surf. Sci.* **55**, 43 (1992).
- <sup>123</sup>A. M. Venezia, A. Rossi, D. Duca, A. Martorana, G. Deganello, *Appl. Catal., A* **125**, 113 (1995).
- <sup>124</sup>G. Deganello, D. Duca, A. Martorana, G. Fagherazzi, A. Benedetti, *J. Catal.* **150**, 127 (1994).
- <sup>125</sup>A. G. Shard, *J. Phys. Chem. C.* **116**, 16806 (2012).
- <sup>126</sup>W. Smekal, W. S. M. Werner, C. J. Powell, *Surf. Interface Anal.* **37**, 1059 (2005).
- <sup>127</sup>M. Chudzicki, W. S. Werner, A. G. Shard, Y. C. Wang, D. G. Castner, C. J. Powell, *J. Phys Chem C Nanomater Interfaces* **119**, 17687 (2015).

- <sup>128</sup>M. Chudzicki, W. S. M. Werner, A. G. Shard, Y. C. Wang, D. G. Castner, C. J. Powell, *J. Phys. Chem. C* **120**, 2484 (2016).
- <sup>129</sup>M. J. Edgell, R. W. Paynter, J. E. Castle, *J. Electron Spectrosc. Relat. Phenom.* **37**, 241 (1985).
- <sup>130</sup>J. E. Castle, L. B. Hazell, R. D. Whitehead, *J. Electron Spectrosc. Relat. Phenom.* **9**, 247 (1976).
- <sup>131</sup>C. D. Wagner, *J. Vac. Sci. Technol.* **15**, 518 (1978).
- <sup>132</sup>J. E. Castle, R. H. West, *J. Electron Spectrosc. Relat. Phenom.* **19**, 409 (1980).
- <sup>133</sup>S. Diplas, J. F. Watts, S. A. Morton, G. Beamson, P. Tsakiropoulos, D. T. Clark, J. E. Castle, *J. Electron Spectrosc. Relat. Phenom.* **113**, 153 (2001).
- <sup>134</sup>A. G. Shard, J. D. P. Counsell, D. J. H. Cant, E. F. Smith, P. Navabpour, X. Zhang, C. J. Blomfield, *Surf. Interface Anal.* **51**, 763 (2019).
- <sup>135</sup>S. R. Bare, A. Knop-Gericke, D. Teschner, M. Hävacker, R. Blume, T. Rocha, R. Schlögl, A. S. Y. Chan, N. Blackwell, M. E. Charochak, R. ter Veen, H. H. Brongersma, *Surf. Sci.* **648**, 376 (2016).
- <sup>136</sup>C. Song, A. Tayal, O. Seo, J. Kim, Y. Chen, S. Hiroi, L. S. R. Kumara, K. Kusada, H. Kobayashi, H. Kitagawa, O. Sakata, *Nanoscale Adv.* **1**, 546 (2019).
- <sup>137</sup>S. Tougaard, *J. Surf. Anal.* **24**, 107 (2017).
- <sup>138</sup>C. Zborowski, S. Tougaard, *Surf. Interface Anal.* **51**, 857 (2019).
- <sup>139</sup>P. Risterucci, O. Renault, E. Martinez, B. Detlefs, J. Zegenhagen, G. Grenet, S. Tougaard, *Surf. Interface Anal.* **46**, 906 (2014).